

# Magneto-convection in Chiral Fluid with Variation of Viscosity through a Saturated Porous Media in the Presence of Coriolis Force

<sup>1</sup>Sujatha.N, <sup>2</sup>Mallika.K.S, <sup>3</sup>Nagaraju

<sup>1</sup>Assistant Professor, Department of Mathematics, B.M.S. College of Engineering, Bengaluru-560 019, India.

<sup>2</sup>Associate Professor, Department of Mathematics, Global Academy of Technology, Bengaluru – 560098, India.

<sup>3</sup>Associate Professor, Department of Mechanical Engineering, Siddaganga Institutes Technology, Tumkuru-573103, India.

## Abstract

The effects of variation of viscosity and coriolis force on Oberbeck magneto-convection of a chiral fluid in the presence of the transverse magnetic field, viscous dissipation with saturated porous media are investigated. The coupled non-linear ordinary differential equations governing the flow and heat transfer characteristics of the problem are solved both analytically and numerically. The analytical solutions are obtained using a regular perturbation and numerical solutions obtained using finite difference method. The solution is valid for small values of Buoyancy parameter and variable viscosity parameter. The analytical results are compared with the numerical results and found good agreement. The role of temperature dependent viscosity and viscous dissipation on velocity, temperature, skin friction and the rate of heat transfer are determined. The results are depicted graphically.

**Keywords** - Chiral fluid, Coriolis force, Regular perturbation, Finite difference method

## I. INTRODUCTION

The study of flow problems which involve the interaction of several phenomena, has a wide range of applications in the field of science and technology. There are several transport processes in industry and in nature where buoyancy force arise from both thermal and mass diffusion caused by the temperature gradients and the concentration difference of dissimilar chemical species. Hence, this analysis deal with the free convection flows driven by temperature gradients and concentration differences. When the free convection occurs at high temperatures, radiation effects, Soret effect i.e., thermal diffusion, variation of viscosity with temperature and variation of thermal conductivity of the fluid cannot be neglected. Nuclear power plants, missiles, gas turbines and space vehicles are the examples of such engineering areas.

The Reddy et.al [1] studied unsteady magneto-hydrodynamics convective heat and mass transfer flow past a semi-infinite vertical porous plate with

variable viscosity and thermal conductivity. They assumed that viscosity of the fluid varies as an inverse linear function of temperature. Free convection can have significant effects on forced flows over solid bodies. It can alter the flow field and hence the heat transfer rate and the wall shear stress. Such effects are particularly enhanced for high-speed rotating medium is important due to its application in many areas of geophysics, astrophysics and fluid engineering. Taking into account this fact, the author A. K. Singh had investigated MHD free convection flow past an infinite vertical isothermal porous plate started impulsively in its own plane in a rotating system.

N.Nanousis[6] considered MHD free convective and mass transfer flow past a moving infinite vertical isothermal plate in a rotating fluid taking into account the thermal plate in a interest in heat transfer problems for a non-Newtonian fluid has grown persistently in the past half century. In porous media, the effect of viscosity variation was considered [7],[8] & [8] and studied the thermal diffusion effects on free convective heat and mass transfer flow over an infinite vertical moving plate and noticed that fluid velocity rises due to greater thermal diffusion.

A chiral material characterized by either left handed or right handed, is a type of molecule that lacks an internal plane of symmetry and has a non-superimposable with its mirror image by any amount of rotation and [2] & [3]. Rudraiah et al., [11],[12],[13],[14] & [15] have studied the effect of variation of viscosity on Oberbeck magneto-convection in a chiral fluid in the presence of coriolis force, viscous dissipation and chemical reaction. The objective of the present study is to investigate the Oberbeck convective flow in a vertical chiral fluid layer with variable viscosity and coriolis force with saturated porous media. Analytical solutions of the coupled non-linear momentum and energy equations are obtained using a regular perturbation method. To know the validity of analytical solution, the numerical solution is obtained using the finite difference scheme

with SOR The velocity, temperature, skin friction and rate of heat transfer are computed and the results obtained are depicted graphically.

II. MATHEMATICAL FORMULATION

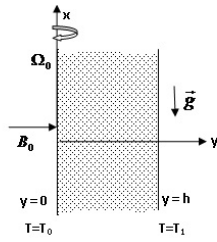


Fig-1: Physical configuration

consider a physical configuration as shown in Fig-1 which consists of an incompressible Boussinesq chiral fluid saturating an infinite vertical sparsely packed porous layer of width  $h$ . A Cartesian frame of reference is chosen with  $x$  and  $y$  axes in the vertical and horizontal directions respectively. A uniform magnetic field  $B_0$  and rotation  $\Omega_0$  are applied in the  $y$  direction which is perpendicular to both  $x$  and  $y$  axes. The flow in the porous medium is governed by the Darcy-Brinkman equation with effective viscosity.

The mass conservation equation for an incompressible Boussinesq chiral fluid is:

$$\nabla \cdot \vec{q} = 0, \tag{1}$$

Equation of state for a Boussinesq fluid is:

$$\rho = \rho_0(1 - \alpha_2(T - T_0)), \tag{2}$$

Conservation of momentum in the presence of Lorentz force,  $\vec{J} \times \vec{B}$  is:

$$\rho_0 \left[ \frac{\partial \vec{q}}{\partial t} + (\vec{q} \cdot \nabla) \vec{q} - 2(\vec{q} \times \vec{\Omega}) \right] = -\nabla p + \rho \vec{g} + \mu_f \nabla^2 \vec{q} + \vec{J} \times \vec{B} - \frac{\mu}{k'} \vec{q}, \tag{3}$$

Conservation of energy in the presence of viscous dissipation  $\phi$  is:

$$\rho_0 c_p \left[ \frac{\partial T}{\partial t} + (\vec{q} \cdot \nabla) T \right] = k \nabla^2 T + \phi, \tag{4}$$

where

$$\phi = 2\mu_f \left[ \left( \frac{\partial u}{\partial x} \right)^2 + \left( \frac{\partial v}{\partial y} \right)^2 + \left( \frac{\partial w}{\partial z} \right)^2 + \frac{1}{2} \left( \frac{\partial u}{\partial y} + \frac{\partial v}{\partial x} \right)^2 + \frac{1}{2} \left( \frac{\partial v}{\partial z} + \frac{\partial w}{\partial y} \right)^2 + \frac{1}{2} \left( \frac{\partial w}{\partial x} + \frac{\partial u}{\partial z} \right)^2 \right]$$

conservation of electric charges in the presence of convective current

$$\vec{J} = \rho_e \vec{q} \tag{5}$$

where the displacement current  $\partial \vec{D} / \partial t$  is neglected compared to convective current  $\rho_e \vec{q}$

$$\frac{\partial \rho_e}{\partial t} + \nabla \cdot (\rho_e \vec{q}) = 0, \tag{6}$$

The constitutive equations for chiral fluids following Rudraiah et.al (2000) and Varadan et.al (1989)

$$\vec{D} = \epsilon \vec{E} + i\gamma \vec{B}, \tag{7}$$

$$\vec{B} = \mu_m \vec{H} - i\mu_m \gamma \vec{E}, \tag{8}$$

The viscosity of chiral fluid is assumed to be temperature dependent and is of the form

$$\mu = \mu_0(1 - \alpha_1(T - T_0)). \tag{9}$$

The flow is assumed to be fully developed, steady and unidirectional parallel to  $x$  axis(see Fig.1), so that all the physical quantities vary only w.r.t  $y$  except the pressure,  $p$ . The hydrostatic balance is  $-\partial p / \partial x = \rho_0 g$ .

Under these assumptions, equations (1) to (4) respectively take the form

$$\frac{\partial v}{\partial y} = 0 \Rightarrow v = v_0 \tag{10}$$

$$v_0 \left( 1 - \alpha_1(T - T_0) \right) \frac{d^2 u}{dy^2} - v_0 \alpha_1 \frac{du}{dy} \frac{dT}{dy} - v_0 \frac{du}{dy} - \frac{v_0}{\kappa'} u + \alpha_1(T - T_0) g + \frac{\rho_e v_0 B_0}{\rho_0} + 2v_0 \Omega_0 = 0, \tag{11}$$

$$k \frac{d^2 T}{dy^2} - \rho_0 c_p v_0 \frac{dT}{dy} + \mu_0 \left( \frac{du}{dy} \right)^2 - \mu_0 \alpha_1(T - T_0) \left( \frac{du}{dy} \right)^2 = 0 \tag{12}$$

From equation (6) using equation (1) and also using the assumption become

$$\rho_e = \text{constant} \tag{13}$$

The following non- dimensional variables are used to make equations (11) and (12) non dimensional following Rudraiah et.al [2] & [3].

$$y^* = \frac{y}{h}, u^* = \frac{u}{\alpha_2 g h^2 \Delta T / \nu}, \rho_e^* = \frac{\rho_e}{(\epsilon^2 E_0^2 + \gamma^2 B_0^2) \nu / h^2}$$

$$\theta = \frac{T - T_0}{\Delta T}, \Delta T = T_1 - T_0 \tag{14}$$

The non-dimensional form of the governing equations (11) and (12) using equation (14) after neglecting the asterisks, are:

$$(1 - R_1 \theta) \frac{d^2 u}{dy^2} - R_1 \frac{du}{dy} \frac{d\theta}{dy} - \text{Re} \frac{du}{dy} - \sigma^2 u + \theta + \frac{M \text{Re}}{Gr} + \frac{\sqrt{Ta} \text{Re}}{Gr} = 0, \quad (15)$$

$$\frac{d^2 \theta}{dy^2} - Pe \frac{d\theta}{dy} + N(1 - R_1 \theta) \left( \frac{du}{dy} \right)^2 = 0 \quad (16)$$

Here  $R_1 = \alpha_1 \Delta T$ , viscosity variation coefficient,  $\text{Re} = v_0 h / \nu$ , the Reynolds number,  $M = (B_0 (\epsilon^2 E_0^2 + \gamma^2 B_0^2) \nu \rho_e) / v_0 \rho_0$ , the magnetochiral number,  $Gr = g \beta \nu \Delta T / v_0^3$ , the Grashof number,  $Pe = v_0 h / K$ , the Peclet number,  $N = \rho_0 \alpha_0^2 g^2 h^4 \Delta T / v_0 k$ , the buoyancy parameter,  $\sigma = h^2 / \sqrt{k}$ , porous parameter and  $Ta = 4\Omega_0^2 h^4 / v_0^2$ , the Taylor number.

Making the no-slip and isothermal boundary conditions on velocity and temperature dimensionless using equation (14), we get

$$u = 0, \text{ at } y = 0, \quad u = 0, \text{ at } y = 1 \quad (17)$$

$$\theta = 0 \text{ at } y = 0, \quad \theta = 1 \text{ at } y = 1 \quad (18)$$

### III. ANALYTICAL SOLUTION

Equations (15) and (16) are the coupled non-linear differential equations, whose analytical Solutions are obtained using a regular perturbation technique with Buoyancy parameter  $N$  as a perturbation parameter. In this technique  $u$  and  $\theta$  are expressed in a series form, given by

$$u = u_0 + N u_1 + N^2 u_2 + \dots \quad (19)$$

$$\theta = \theta_0 + N \theta_1 + N^2 \theta_2 + \dots \quad (20)$$

subjected to satisfying the boundary conditions (17) and (18). Substituting equations (19) and (20) into equations (15) and (16) and equating the like powers of  $N$  to zero we obtain

Zeroth order equations:

$$\frac{d^2 \theta_0}{dy^2} - Pe \frac{d\theta_0}{dy} = 0 \quad (21)$$

$$(1 - R_1 \theta_0) \frac{d^2 u_0}{dy^2} - R_1 \frac{du_0}{dy} \frac{d\theta_0}{dy} - \text{Re} \frac{du_0}{dy} - \sigma^2 u_0 = 0$$

$$= -\theta_0 - \frac{M \text{Re}}{Gr} - \frac{\text{Re} \sqrt{Ta}}{Gr}. \quad (22)$$

First order equations:

$$\frac{d^2 \theta_1}{dy^2} - Pe \frac{d\theta_1}{dy} + (1 - R_1 \theta_0) \left( \frac{du_0}{dy} \right)^2 = 0, \quad (23)$$

$$(1 - R_1 \theta_0) \frac{d^2 u_1}{dy^2} - \text{Re} \frac{du_1}{dy} \frac{d\theta_0}{dy} - R_1 \theta_1 \frac{d^2 u_0}{dy^2} - R_1 \frac{du_0}{dy} \frac{d\theta_1}{dy} - \text{Re} \frac{du_1}{dy} - \sigma^2 u_1 = -\theta_1. \quad (24)$$

The solution of eqn. (21), satisfying the boundary conditions (18) is

$$\theta_0 = A_1 + A_2 e^{Pe y} \quad (25)$$

Equations (22) to (24) are differential equations with variable coefficients; it is difficult to find the solutions. To overcome this difficulty, we again use regular perturbation technique with  $R_1$  as a perturbation parameter and  $u_0$  and  $u_1$  take the form

$$u_0 = u_{00} + R_1 u_{01}, \quad (26)$$

$$u_1 = u_{10} + R_1 u_{11}, \quad (27)$$

with  $R_1$  as a very small parameter.

Equation (22) and (24), using equations (26) and (27) and equating like power to zero, we get

Zeroth order equations:

$$\frac{d^2 u_{00}}{dy^2} - \text{Re} \frac{du_{00}}{dy} - \sigma^2 u_{00} + \theta_0 + \frac{M \text{Re}}{Gr} + \frac{\sqrt{Ta} \text{Re}}{Gr} = 0 \quad (28)$$

$$\frac{d^2 u_{10}}{dy^2} - \text{Re} \frac{du_{10}}{dy} - \sigma^2 u_{10} + \theta_1 = 0 \quad (29)$$

First order equations:

$$\frac{d^2 u_{01}}{dy^2} - \text{Re} \frac{du_{01}}{dy} - \sigma^2 u_{01} - \theta_0 \frac{d^2 u_{00}}{dy^2} - \frac{d\theta_0}{dy} \frac{du_{00}}{dy} = 0, \quad (30)$$

$$\frac{d^2 u_{11}}{dy^2} - \theta_0 \frac{d^2 u_{10}}{dy^2} - \theta_1 \frac{d^2 u_0}{dy^2} - \text{Re} \frac{du_{11}}{dy} - \frac{d\theta_0}{dy} \frac{du_{10}}{dy} - \frac{d\theta_1}{dy} \frac{du_0}{dy} - \sigma^2 u_{11} = 0. \quad (31)$$

In this study, we restrict our solution to the first order approximation. Validity of this approximation will be done using numerical technique.

The solutions of the ordinary differential equations (28) and (30) respectively, using equation (25), subject to satisfying the boundary conditions (17) and (18), are

$$u_{00} = a_0 + a_1 y + a_2 e^{Pe y} + A_4 e^{Re y} \quad (32)$$

$$u_{01} = a_3 + a_4 e^{Pe y} + a_5 e^{2Pe y} + a_6 e^{(Pe+Re)y} + a_7 y e^{Re y} \quad (33)$$

$$u_0 = u_{00} + R_1 u_{01} \quad (34)$$

The solution of equation (23), using equations (25) and (34), is

$$\theta_1 = a_8 + a_9 y + A_8 e^{Pe y} + a_{10} e^{2Pe y} + a_{11} e^{3Pe y} + a_{12} e^{4Pe y} + a_{13} e^{5Pe y} + a_{14} e^{Re y} + a_{15} e^{2Re y} + a_{16} e^{(Pe+Re)y} + a_{17} e^{(Pe+2Re)y} + a_{18} e^{(2Pe+Re)y} + a_{19} e^{(2Pe+2Re)y} + a_{20} e^{(3Pe+Re)y} + a_{21} e^{(4Pe+Re)y} + a_{22} e^{(3Pe+4Re)y} + a_{23} y e^{Pe y} + a_{24} y e^{Re y} + a_{25} y e^{2Re y} + a_{26} y e^{(2Pe+2Re)y} + a_{27} y e^{(Pe+2Re)y} + a_{28} y e^{(2Pe+Re)y} + a_{29} y^2 e^{2Re y} + a_{30} y^2 e^{(Pe+2Re)y} + a_{31} e^{(Pe+Re)y} \quad (35)$$

Equations (29) and (31) are the ordinary differential equations whose solutions using equations. (25), (34) and (35), are

$$u_{10} = A_9 + a_{32} y + a_{33} y^2 + a_{34} e^{Pe y} + a_{35} e^{Re y} - a_{36} e^{2Pe y} - a_{37} e^{3Pe y} + a_{38} e^{4Pe y} + a_{39} e^{5Pe y} - a_{40} e^{(4Pe+Re)y} - a_{41} e^{(3Pe+4Re)y} + a_{42} e^{2(Pe+Re)y} + a_{43} e^{(2Pe+Re)y} + a_{44} e^{(Pe+2Re)y} + a_{45} e^{(Pe+2Re)y} + a_{46} e^{(Pe+Re)y} + a_{47} y e^{Pe y} + a_{48} y e^{Re y} + a_{49} y e^{2Re y} + a_{50} y e^{(Pe+Re)y} + a_{51} y e^{2(Pe+Re)y} + a_{52} y e^{(2Pe+Re)y} + a_{53} y e^{(Pe+2Re)y} - a_{54} y^2 e^{Re y} - a_{55} y^2 e^{2Re y} + a_{56} y^2 e^{(Pe+2Re)y} , \quad (36)$$

$$u_{11} = A_{11} + a_{57} y + a_{58} e^{Pe y} + a_{59} e^{2Pe y} + a_{60} e^{3Pe y} + a_{61} e^{4Pe y} + a_{62} e^{5Pe y} + a_{63} e^{6Pe y} + a_{64} e^{(4Pe+Re)y} + a_{65} e^{(3Pe+4Re)y} + a_{66} e^{(2Pe+Re)y} + a_{67} e^{(3Pe+2Re)y} + a_{68} e^{(3Pe+Re)y} + a_{69} e^{2(Pe+Re)y} + a_{70} e^{Re y} + a_{71} e^{2Re y} + a_{72} e^{(Pe+Re)y} + a_{73} e^{(Pe+Re)y} + a_{74} e^{4(Pe+Re)y} + a_{75} y e^{Pe y} + a_{76} y e^{2Pe y} + a_{77} y e^{(2Pe+Re)y} + a_{78} y e^{(3Pe+2Re)y} + a_{79} y e^{(3Pe+Re)y} + a_{80} y e^{2(Pe+Re)y} + a_{81} y e^{Re y} + a_{82} y e^{2Re y} + a_{83} y e^{(Pe+Re)y} + a_{84} y e^{(Pe+Re)y} + a_{85} y e^{4(Pe+Re)y} + a_{86} y^2 e^{2Re y} + a_{87} y^2 e^{2Re y} + a_{88} y^2 e^{2Re y} + a_{89} y^2 e^{2(Pe+Re)y} + a_{90} y^2 e^{2(Pe+Re)y} + a_{91} y^2 e^{2(4Pe+Re)y} + a_{92} y^3 e^{3Re y} . \quad (37)$$

$$u_1 = u_{10} + R_1 u_{11} \quad (38)$$

The constants involved in equations (32) to (37) are determined using the boundary conditions. These constants are very lengthy and hence omitted here but they are included in the computation of the solutions.

### A. Skin Friction

In many practical applications involving separation of flow, it is advantageous to know the skin friction and heat transfer at the boundaries. These can be determined once we know the velocity and temperature distributions. The skin friction can be calculated from the shear stress  $\tau$  at the walls defined as

$$\tau = \mu_f \left( \frac{\partial u}{\partial y} \right)$$

The dimensionless expression for skin friction is expressed as

$$\tau = (1 - R_1 \theta) \left( \frac{\partial u}{\partial y} \right) \quad (39)$$

### B.Heat Transfer

The rate of heat transfer between the fluid and the plate is given by

$$q' = -k \left( \frac{\partial T}{\partial Y} \right)$$

where  $q'$  is the heat flux.

The non-dimensional form of heat transfer equations, can be expressed as Nusselt number,  $Nu$ , given by

$$Nu = - \frac{\partial \theta}{\partial y} \quad (40)$$

#### IV. NUMERICAL SOLUTION

To know the validity of analytical solutions obtained using the approximate method of regular perturbation technique, we find in this section the numerical solution of the coupled nonlinear equations (14) to (15) using the second order  $O(h^2)$  central finite difference scheme. After applying the central finite difference scheme, equations (14) and (15) take the form

$$\begin{aligned} & (1 - R_1 \theta_i) \left[ \frac{u_{i+1} - 2u_i + u_{i-1}}{\Delta y} \right] \\ & - \left( \frac{u_{i+1} - u_{i-1}}{2 \Delta y} \right) \left[ Re - R_1 \left( \frac{T_{i+1} - T_{i-1}}{2 \Delta y} \right) \right] \\ & - \sigma^2 u_i + \theta_i + k_1 = 0, \end{aligned} \quad (41)$$

where

$$\begin{aligned} k_1 &= \frac{M Re}{Gr} + \frac{\sqrt{Ta} Re}{Gr} \\ & \frac{\theta_{i+1} - 2\theta_i + \theta_{i-1}}{\Delta y} - Pe \left( \frac{\theta_{i+1} - \theta_{i-1}}{2 \Delta y} \right) \\ & + N (1 - R_1 \theta_i) \left( \frac{u_{i+1} - u_{i-1}}{2 \Delta y} \right)^2 = 0. \end{aligned} \quad (42)$$

Successive over-relaxation has been used for the quick convergence of the solution. The results obtained are discussed and conclusions are drawn in the section VI.

#### V. TABLES AND FIGURES

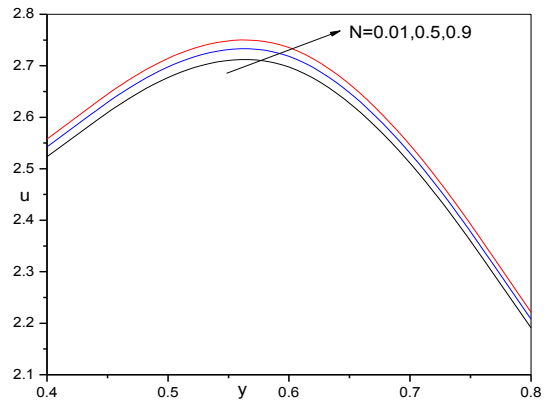


Fig-2: velocity profiles for different values of  $N$

$M = 10, Gr = 1, Re = 2, Ta = 5, Pe = 5, \sigma = 0.01, R_1 = 0.01$

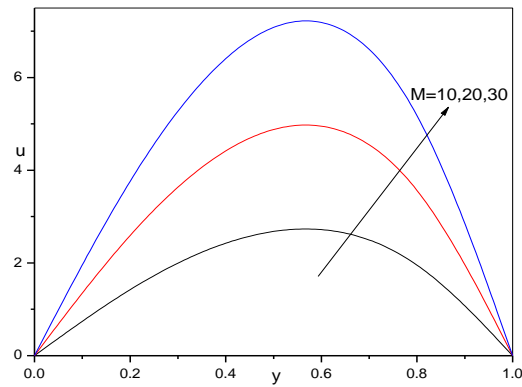


Fig-3: velocity profiles for different values of  $M$

$N = 0.01, Gr = 1, Re = 2, Ta = 5, Pe = 5, \sigma = 0.01, R_1 = 0.01$

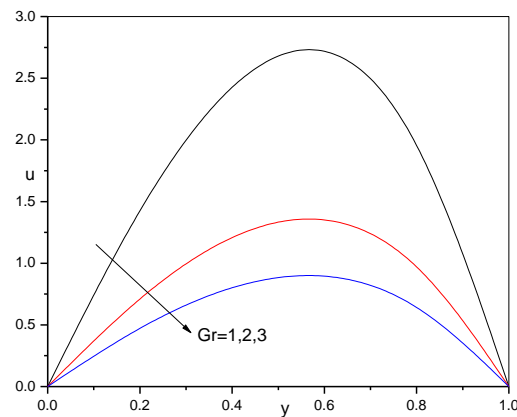
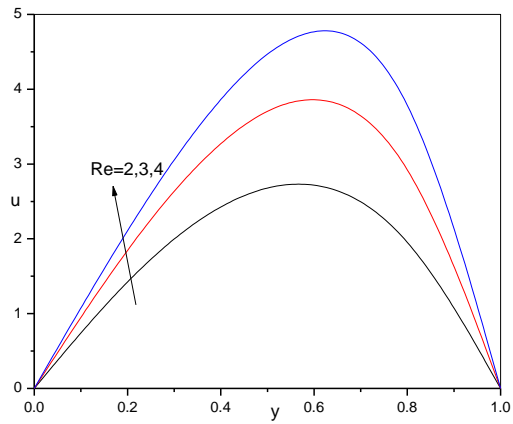


Fig. 4: velocity profiles for different values of  $Gr$  when

$N = 0.01, M = 10, Re = 2, Ta = 5, Pe = 5, \sigma = 0.01, R_1 = 0.01$



**Fig-5: velocity profiles for different values of  $Re$**

$N = 0.01, M = 10, Gr = 1, Ta = 5, Pe = 5, \sigma = 0.01, R_1 = 0.01$

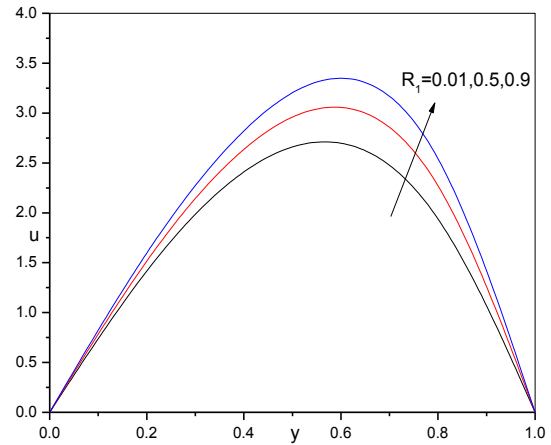


**Fig-8: velocity profiles for different values of  $R_1$  when**

$N = 0.01, M = 10, Gr = 1, Re = 2, Ta = 5, Pe = 5, \sigma = 0.01$

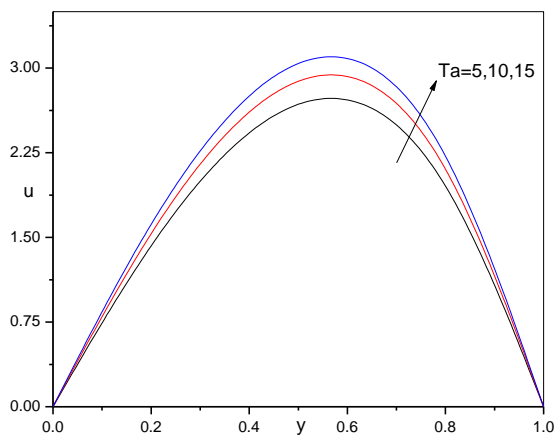


**Fig-6: velocity profiles for different values of  $Ta$**

$N = 0.01, M = 10, Gr = 1, Re = 2, Pe = 5, \sigma = 0.01, R_1 = 0.01$

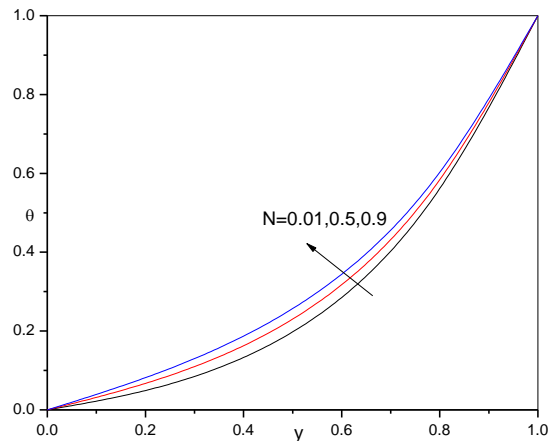


**Fig-9: Temperature profiles for different values of  $N$**

$M = 10, Gr = 1, Re = 2, Ta = 5, Pe = 5, \sigma = 0.01, R_1 = 0.01$

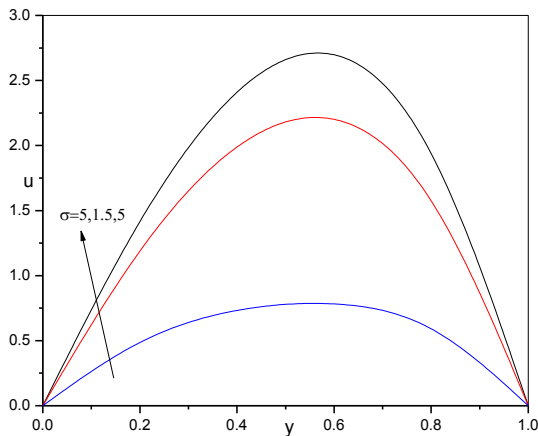


**Fig-7: velocity profiles for different values of  $\sigma$  when**

$N = 0.01, M = 10, Gr = 1, Re = 2, Ta = 5, Pe = 5, R_1 = 0.01$

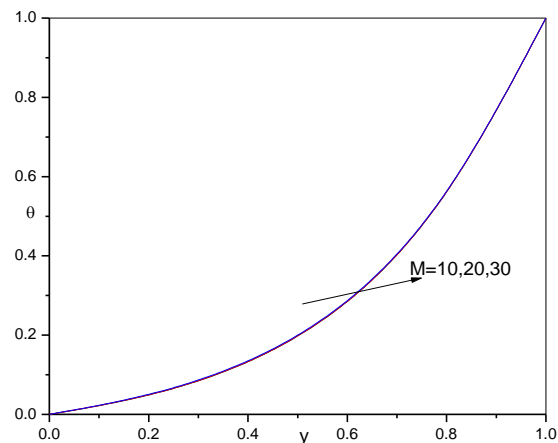


**Fig-10: Temperature profiles for different values of  $M$**

$N = 0.01, Gr = 1, Re = 2, Ta = 5, Pe = 5, \sigma = 0.01, R_1 = 0.01$

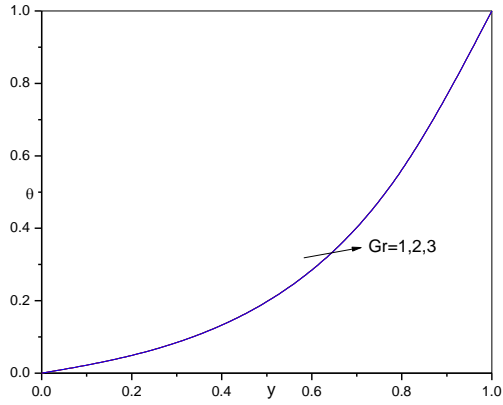


**Fig-11: Temperature profiles for different values of  $Gr$**

$N = 0.01, M = 10, Re = 2, Ta = 5, Pe = 5, \sigma = 0.01, R_1 = 0.01$

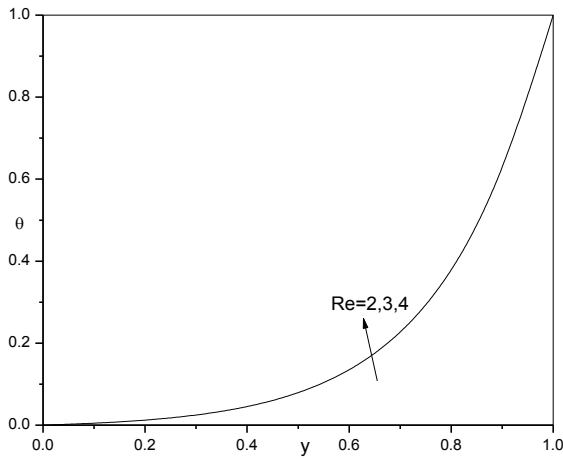


**Fig-12: Temperature profiles for different values of  $Re$**

$N = 0.01, M = 10, Re = 2, Ta = 5, Pe = 5, \sigma = 0.01, R_1 = 0.01$

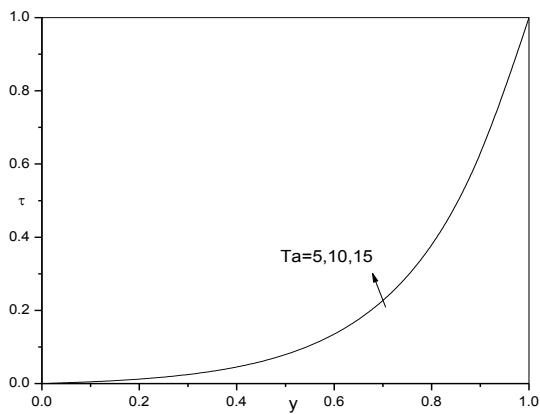


**Fig-13: Temperature profiles for different values of  $Ta$**

$N = 0.01, M = 10, Gr = 1, Re = 2, Pe = 5, \sigma = 0.01, R_1 = 0.01$

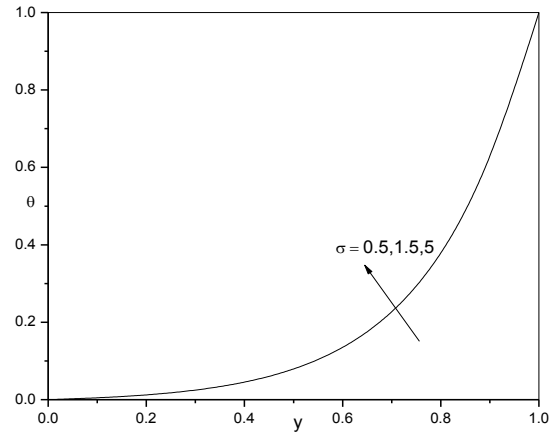


**Fig-14: Temperature profiles for different values of  $\sigma$**

$N = 0.01, M = 10, Gr = 1, Re = 2, Ta = 5, \sigma = 0.01, R_1 = 0.01$

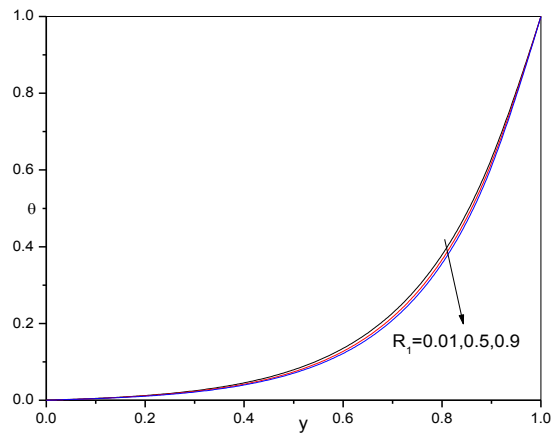


**Fig-15: Temperature profiles for different values of  $R_1$**

$N = 0.01, M = 10, Gr = 1, Re = 2, Ta = 5, Pe = 5, \sigma = 0.01$

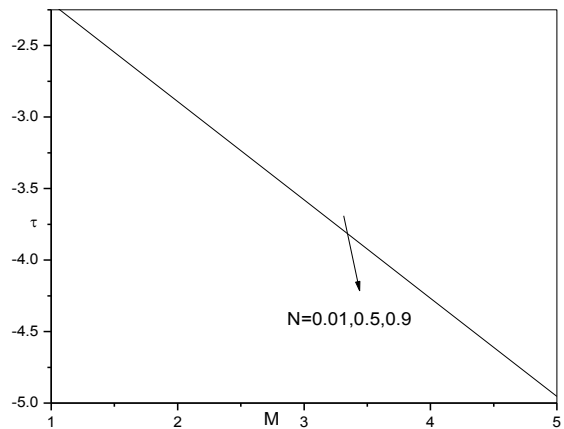


**Fig-16: Skinfriction for various values of  $N$**

$Re = 2, Pe = 5, Gr = 1, Ta = 5, R_1 = 0.01, \sigma = 0.01$

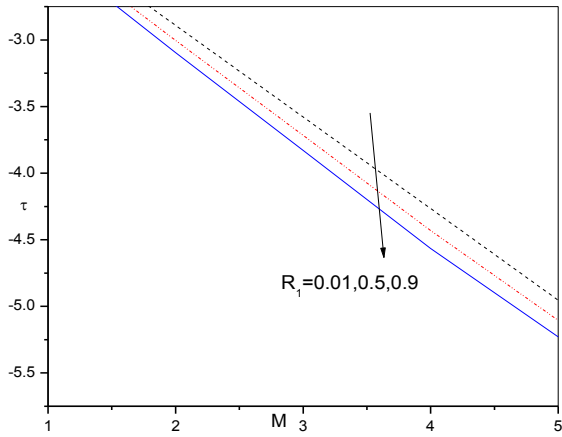


**Fig-17: Skinfriction for various values of  $R_1$**   
 $Re = 2, Pe = 5, Gr = 1, Ta = 5, N = 0.01, \sigma = 0.01$

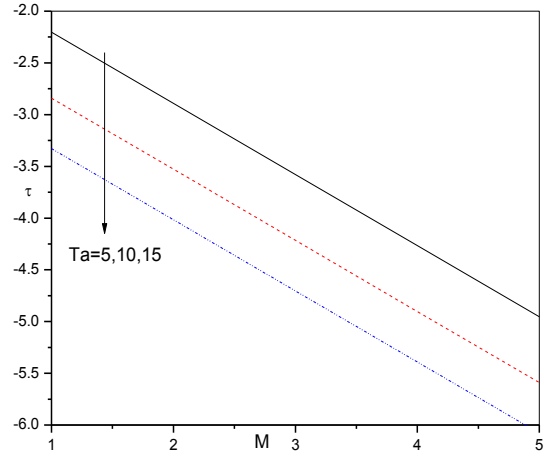


**Fig-20: Skinfriction for various values of  $Ta$**   
 $Re = 2, Pe = 5, Gr = 1, R_1 = 0.01, N = 0.01, \sigma = 0.01$

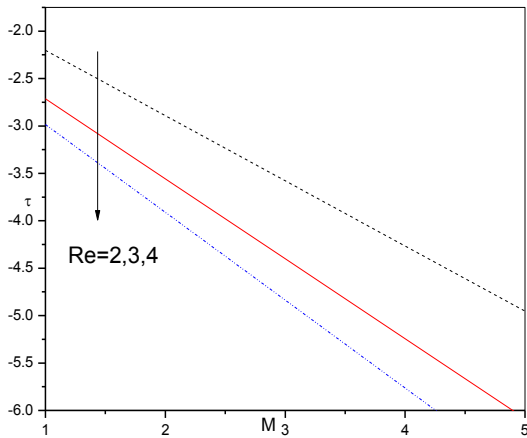


**Fig-18: Skinfriction for various values of  $Re$**   
 $N = 0.01, Pe = 5, Gr = 1, Ta = 5, R_1 = 0.01, \sigma = 0.01$

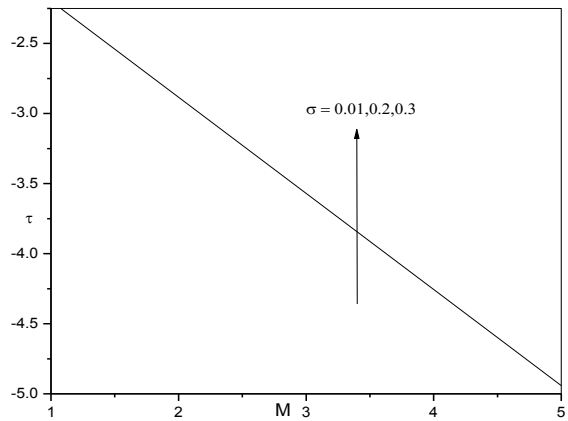


**Fig-21: Skinfriction for various values of  $\sigma$**   
 $Re = 2, Pe = 5, Gr = 1, R_1 = 0.01, N = 0.01, Ta = 5$

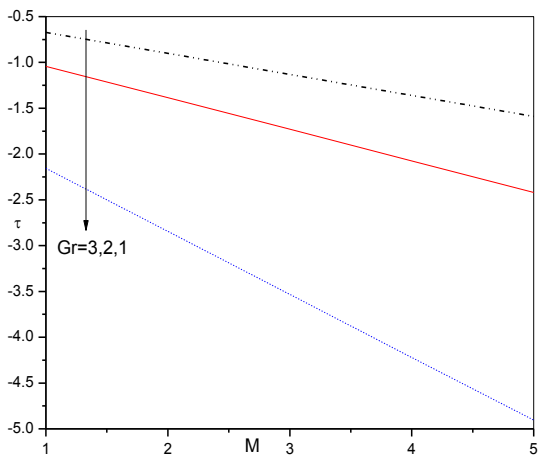


**Fig-19: Skinfriction for various values of  $Gr$**   
 $N = 0.01, Pe = 5, Re = 2, Ta = 5, R_1 = 0.01, \sigma = 0.01$

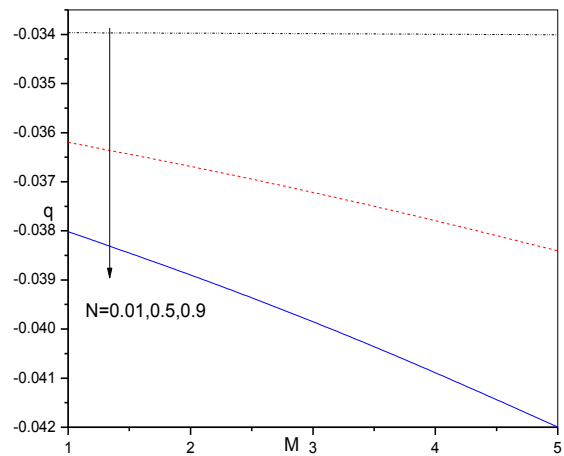


**Fig-22: Heat transfer for various values of  $N$**   
 $Re = 2, Pe = 5, Gr = 1, Ta = 5, R_1 = 0.01, \sigma = 0.01$



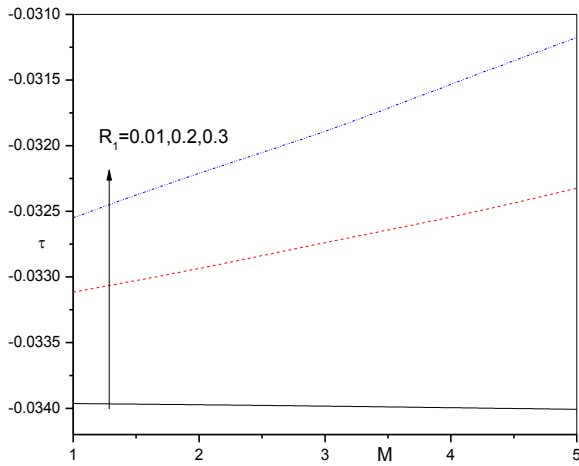


**Fig-23: Heat transfer for various values of  $R_1$**   
 $Re = 2, Pe = 5, Gr = 1, Ta = 5, N = 0.01, \sigma = 0.01$

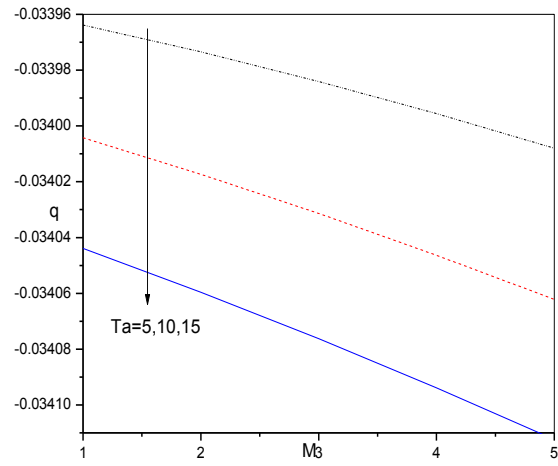


**Fig-26: Heat transfer for various values of  $Ta$**   
 $Re = 2, Pe = 5, Gr = 1, R_1 = 0.01, N = 0.01$

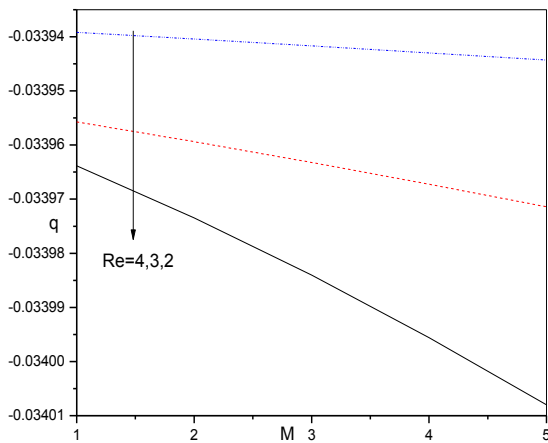


**Fig-24: Heat transfer for various values of  $Re$**   
 $N = 0.01, Pe = 5, Gr = 1, Ta = 5, R_1 = 0.01, \sigma = 0.01$

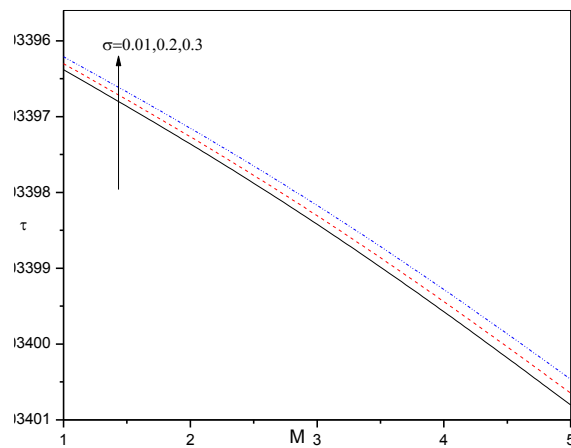


**Fig-27: Heat transfer for various values of  $\sigma$**   
 $Re = 2, Pe = 5, Gr = 1, R_1 = 0.01, N = 0.01, Ta = 5$

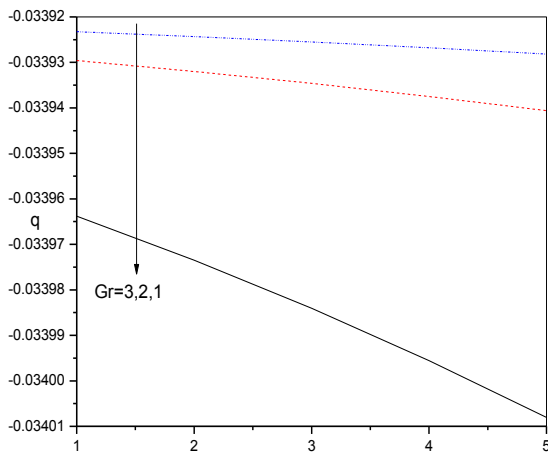


**Fig-25: Heat transfer for various values of  $Gr$**   
 $N = 0.01, Pe = 5, Re = 2, Ta = 5, R_1 = 0.01, \sigma = 0.01$

**Table 1: Comparison of velocity and temperature profiles for different values of Buoyancy parameter**

	Rudraiah et al.[2013]		Present work	
y	u	$\theta$	u	$\theta$
0.0	0.0000	0.0000	0.0000	0.0000
0.2	0.0127	0.0127	0.0122	0.0157
0.4	0.0442	0.0442	0.0428	0.0439
0.6	0.1305	0.1305	0.1300	0.1305
0.8	0.3647	0.3647	0.3666	0.3647
1.0	1.0000	1.0000	1.0000	1.0000

## VI. RESULT AND DISCUSSION

The analytical solutions for effects of variation of viscosity on Oberbeck magneto-convection in a chiral fluid with saturated porous media in the presence of coriolis force are investigated. The results are presented graphically in Figs. (2) to (27).

Comparisons of analytical results with numerical results are performed and excellent agreement found between analytical and numerical results. Non-linear ordinary differential equations are solved analytically using regular perturbation method and numerical solution obtained using finite difference method. Fig. (2) displays the velocity distribution for various values of  $N$ . It is observed from this figure that there is a slight increment in velocity distribution i.e., velocity profile increases with an increasing the buoyancy parameter. Figs. (3),(6) and (8) show the variation of velocity profile for various values of  $M$ ,  $Ta$  and  $R_1$ . It is observed from these figures that the velocity distribution increase in the value of  $M$ ,  $Ta$  and  $R_1$ . Figs. (4),(5) and (7) represent the velocity distribution for various values of  $Gr, Re$  and  $\sigma$ . It is observed from these figures that velocity distributions decrease with an increase in  $Gr, Re$  and  $\sigma$ . The effect of  $\sigma$  is to decrease the velocity profile. This is due to increase in obstruction of the fluid motion with an increase in the  $\sigma$ , thereby increase in the porous parameter indicates decrease in the permeability of the porous medium so the fluid velocity decreases. Fig. (8) displays the variation of velocity distribution for various values of  $R_1$ . It is observed that the velocity distribution increase with increasing  $R_1$ . Figs. (9) to (15) display the variation of temperature distribution  $\theta$  with  $y$  for various values of  $N, M, Gr, Re, Ta, \sigma$  and  $R_1$  respectively. From these figures, it is seen that no significant effects have been found of above mentioned dimensionless parameters on temperature distributions. But the Fig. (9) shows that a small variation in temperature profile for various values of  $N$ . It is Observed from this figure that temperature distribution increases with increasing  $N$ . Figs. (16) to (21) represent the effect of skin-friction with  $M$  for various values of  $N, R_1, Re$  and  $Gr$  respectively. Fig. (16) displays the effect of skin-friction with  $M$  for various values of buoyancy parameter. It is observed from this figure that no variation has been found for various values of  $N$ . Further, it is noted that skin-friction increase in  $M$ . The variation of skin-friction with  $M$  for various values of  $R_1, Re$  and  $Gr$  are depicted in Figs. (17), (18) and (19). From these figures, it is clear that the skin-friction decreases with increase in the values of  $R_1, Re$  and  $Gr$ . Further, it is observed that the skin-friction increases with increasing  $M$ . Fig. (20) represents the variation of skin-friction with  $M$  for various values of  $Ta$ . It is observed from the figure that skin-friction decreases for various values of  $Ta$ . Further, it is observed from that the skin-friction increases with increasing  $M$ . Fig. (21) shows the variation of skin-friction with  $M$  for various values of  $\sigma$ . It is observed that the effects of skin-friction with  $M$  for various values of  $\sigma$ . Further, from this figure, it is seen that skin-friction increases with increase in  $M$ . Figs. (22) to (27) display the variation of rate of heat transfer with magnetochiral number  $M$ , for various values of  $N,$

$R_1, Re, Gr, Ta$  and  $\sigma$  respectively. The effects of  $N, R_1$  and  $Ta$  on skin-friction with  $M$  are presented in Figs. (22), (23) and (26). These graphs illustrate the heat transfer increase with increase in  $N, R_1$  and  $Ta$  respectively. Also, we note that the rate of heat transfer increase with an increase in  $M$ . Figs, (24), (25) and (27) represent the variation of rate of heat transfer with  $M$  for various values of  $Re, Gr$  and  $\sigma$  respectively. It is observed from these figures that the rate of heat transfer decrease with increase in  $Re, Gr$  and  $\sigma$ . Further, it is observed that the heat transfer increase with the increase in  $M$ .

## VII. CONCLUSION

The influence of viscosity variation parameter and coriolis force on Oberbeck magnetoconvection in chiral fluid with saturated porous media is studied analytically and numerically. Computed results are presented to exhibit their dependence on the important physical parameters.

We conclude the results as follows:

- Increase in magnetochiral number ( $M$ ), buoyancy parameter ( $N$ ) and Reynolds number ( $Re$ ), increases the magnitude of velocity distribution.
- Increase in viscosity variation parameters ( $R_1$ ) and Reynolds number ( $Re$ ), decrease the magnitude of velocity distribution.
- The increase in magnetochiral number ( $M$ ) and Reynolds number ( $Re$ ), increase the skin friction.
- Increase in viscosity variation parameter ( $R_1$ ) Taylor's number ( $Ta$ ) and Grashof number ( $Gr$ ) decrease the skin friction.
- The increase in magnetochiral number ( $M$ ) and Reynolds number ( $Re$ ), decreases the heat transfer.
- Increase in viscosity variation parameter ( $R_1$ ), increases the heat transfer.
- Increase in Taylor's number ( $Ta$ ), porous parameter ( $\sigma$ ) increase the heat transfer.

## ACKNOWLEDGEMENTS

All three authors are gratefully acknowledges The Principal and the management of BMSCE, Bengaluru, Global Institute of Technology, Bengaluru & Siddaganga Institute of Technology, Tumakuru for providing the environment to carry out this research work.

## REFERENCE

- [1] M.G.Reddy, N. B. Reddy and B. R. Reddy, "Unsteady MHD convective heat and mass transfer flow past a semi-infinite vertical porous plate with variable viscosity and thermal conductivity", Int. J. of Appl. Math and Mech., 5(6):1-14, 2009.
- [2] N.Rudraiah, M. Vekatachalappa, A. A.Natarajan, Basavaraju, "Field equations in Chiral Material and Eddy current losses in transformers", Proc. INSA Conference on Math and its applications to Industry, 1-21, 2000.
- [3] N.Rudraiah, M. L. Sudheer and G. K. Suresh, "Effect of external constraint of magnetic field and velocity shear on

- the propagation of internal waves in chiral fluid”, J. Appl. Fluid Mechanics, 4(1) 115-122, 2010.
- [4] V.K. Varadan and V.V. Varadan, Laktakia, A “Time Harmonic Electromagnetic Fields in Chiral Media”, Springer, 1989.
- [5] A.K. Singh, “MHD free convection flow in the stokes problem for a vertical porous plate in a rotating system”, Astrophys. Space Sci., 95:283–289, 1983.
- [6] N. Nanousis, “Thermal diffusion effects on MHD free convective and mass transfer flow past a moving infinite vertical plate in a rotating fluid”, Astrophys. Space Sci., 191:313–322, 1992.
- [7] N.K. Mehta and S. Sood . “Transient free convection flow with temperature dependent viscosity in a fluid saturated porous media”. Int. J. Eng. Sci., 30:1083–1087, 1992.
- [8] Molla Md. Mamun, Hossain Md. Anwar, and Gorla RSR “Natural convection flow from an isothermal horizontal circular cylinder with temperature dependent viscosity”, Heat Mass Transfer, 41:594-598, 2005.
- [9] N.G. Kafoussius, “MHD thermal diffusion effects on free convection and mass transfer flow over an infinite vertical moving plate”. Astrophysics Space Sci., 192:11–19, 1992.
- [10] Naseer S Elgazery, “Transient analysis of heat and mass transfer by natural convection in power law fluid past a vertical plate immersed in a porous medium” Applications and Applied Mathematics, 3(2):267–285, 2008.
- [11] N. Rudraiah, Sujatha N. and S.V. Raghunatha Reddy “ Effects of temperature dependent viscosity and coriolis force on Oberbeck convection in a chiral fluid in the presence of a transverse magnetic field”, Int. J. Fluid Mech., Vol. 4, No. 2, 183 – 200, 2012.
- [12] N. Rudraiah, Sujatha N. and S.V. Raghunatha Reddy, “Double diffusive Oberbeck convection in a chiral fluid in the presence of chemical reaction and thermal radiation, Int. J. Appl. Math. and Engg. Sci., Vol. 6, No.1, 105 – 116, 2012b.
- [13] N. Rudraiah and Sujatha N., “Radiation effects on Oberbeck double diffusive convection in a chiral fluid in the presence of a transverse magnetic field”, American J. Pure and Appl. Math., Vol. 1, 1 – 12, 2012c.
- [14] N. Rudraiah, Sujatha N. and S.V. Raghunatha Reddy, “Effects of viscous dissipation and an imposed magnetic field on double diffusive Oberbeck convection in a chiral fluid with saturated vertical porous media”, Int. J. Appl. Math. and Engg. Sci., Vol. 6, No.1, 117 – 131, 2012d.
- [15] N. Rudraiah, Sujatha N. and Sofen Kumar Jena, “ Effects of variation of viscosity and viscous dissipation on Oberbeck magnetoconvection in a chiral fluid in the presence of a transverse magnetic field”, J. Appl. Fluid Mech., Vol. 6, No. 2, 229 – 237.